Production of Propene from *n*-Butanol: A Three-Step Cascade Utilizing the Cytochrome P450 Fatty Acid Decarboxylase $OleT_{JE}$

Daniel Bauer[+,[a]] Ioannis Zachos[+,[a]] and Volker Sieber*[a, b, c, d]

Propene is one of the most important starting materials in the chemical industry. Herein, we report an enzymatic cascade reaction for the biocatalytic production of propene starting from *n*-butanol, thus offering a biobased production from glucose. In order to create an efficient system, we faced the issue of an optimal cofactor supply for the fatty acid decarboxylase $OleT_{JE}$, which is said to be driven by either NAD(P)H or H_2O_2. In the first system, we used an alcohol and aldehyde dehydrogenase coupled to $OleT_{JE}$ by the electron-transfer complex putidaredoxin reductase/putidaredoxin, allowing regeneration of the NAD^+ cofactor. With the second system, we intended full oxidation of *n*-butanol to butyric acid, generating one equivalent of H_2O_2 that can be used for the oxidative decarboxylation. As the optimal substrate is a long-chain fatty acid, we also tried to create an improved variant for the decarboxylation of butyric acid by using rational protein design. Within a mutational study with 57 designed mutants, we generated the mutant $OleT_{V292I}$, which showed a 2.4-fold improvement in propene production in our H_2O_2-driven cascade system and reached total turnover numbers >1000.

Introduction

Material use of renewable resources represents one of the most promising ways of overcoming general global challenges, such as the growing demand on oil and gas. The field has gradually broadened as we face a difficult future with irreversibly decreasing fossil fuel reserves and increasing environmental concerns like global warming.[1] The use of alternative and sustainable processes is desirable for nearly all industrial sectors. The established petroleum-based industry in particular needs to meet the demand for a sustainable future. Therefore, "green" and innovative solutions for production of bulk chemicals and "drop-in" compatible fuels as well as niche products need to be developed. Promising starting points for achieving this goal are biomass-based materials (e.g., sugars and fatty acids) that are sustainably available, for example, from lignocellulose or phototrophic organisms. In the case of sugars, recent studies have demonstrated successful *in vitro* bioconversion of glucose to form different alcohols like ethanol,[2] isopropanol[3] and *n*-butanol,[4] which all are excellent molecular platforms for producing bulk commodities.

Additionally, fatty acids derived from biological resources like plants or microorganisms are important raw materials with high potential,[5] for example, for the transformation to alkenes, which are ideal platform molecules. As of recently, this class of molecules can be produced enzymatically starting from fatty acids, such as the FAD-containing fatty acid photodecarboxylase from *Chlorella variabilis* NC64A,[6] or the non-heme-iron oxidase UndA[7] and the desaturase-like enzyme UndB[8] from *Pseudomonas*. In 2011, Rude et al. reported the fatty acid decarboxylase $OleT_{JE}$ (CYP152L1) from *Jeotgalicoccus* sp. ATCC 8456 as being the first cytochrome P450 peroxygenase predominantly decarboxylating fatty acids using just H_2O_2 as cosubstrate.[9] Interestingly, later results showed much higher total turnover numbers (TTN) when using O_2 as an oxidant and NAD(P)H as an electron donor in combination with several redox partners, thus indicating that $OleT_{JE}$ also can act as a monooxygenase.[10–16] Recent studies refuted this theory again and showed a single activity based on decoupling processes.[17] Although initial studies with this enzyme only showed success with long- to medium-chain fatty acids,[9,10,15,18,19,20,21,22] the substrate scope could be widened to a variety of non-native substrates,[23] as well as carboxy compounds[12,14,16,24,25] down to C_4 fatty acids,[11] leading to decarboxylated, hydroxylated and desaturated products. Besides $OleT_{JE}$, further olefin-producing CYP152 peroxygenases have been found in recent years (i.e.,

[a] D. Bauer,[+] I. Zachos,[+] Prof. Dr. V. Sieber
Chair of Chemistry of Biogenic Resources
Campus Straubing for Biotechnology and Sustainability, Technical University of Munich
Schulgasse 16, 94315 Straubing (Germany)
E-mail: sieber@tum.de
[b] Prof. Dr. V. Sieber
TUM Catalysis Research Center
Technical University of Munich
Ernst-Otto-Fischer-Straße 1, 85748 Garching (Germany)
[c] Prof. Dr. V. Sieber
Bio, Electro and Chemocatalysis BioCat, Straubing Branch
Fraunhofer Institute for Interfacial Engineering and Biotechnology IGB
Schulgasse 11a, 94315 Straubing (Germany)
[d] Prof. Dr. V. Sieber
School of Chemistry and Molecular Biosciences, Chemistry Building 68
The University of Queensland
Cooper Road, St. Lucia 4072, Queensland (Australia)
[+] These authors contributed equally to this work.

Supporting information for this article is available on the WWW under https://doi.org/10.1002/cbic.202000378

CYP-Sm46Δ29 from *Staphylococcus massiliensis* S46,[26] $OleT_{MC}$ from *Macrococcus caseolyticus*,[27] $OleT_{JH}$ from *Jeotgalicoccus halophilus*,[28] $OleT_{SQ}$ from *Salinicoccus qingdaonensis*,[28] $OleT_{SA}$ from *Staphylococcus aureus*[28]), whereby the early CYP152 family members and other homologues predominantly catalyze the hydroxylation instead of the decarboxylation of medium- to long-chain fatty acids (i.e., $P450_{SP\alpha}$ from *Sphingomonas paucimobilis*,[29] $P450_{BS\beta}$ from *Bacillus subtilis*,[30] $P450_{CLA}$ from *Clostridium acetobutylicum*,[31] CYP-Aa162 from *Alicyclobacillus acidocaldarius* LAA1,[26] CYP-MP from *Methylobacterium populi*[32]).

In this study, we focus on the production of propene, which, with an annual production of 80 million tons, is the most important olefin other than ethylene in the chemical industry.[33] It is assumed that the global demand for propene will increase to 165 million tons per year by 2030, which is about 12–14% more than the amount of propene that can be produced by conventional methods.[34] Currently, propene is still predominantly produced through steam cracking of hydrocarbons, despite the decrease in fossil resources and global warming.[33] However, bio-based propene is already being produced from sugar cane by chemical conversion of bioethanol and ethylene.[35] Propene can also be produced by enzymatic conversion starting from *n*-butanol using the oxidative decarboxylase $OleT_{JE}$ for the last step. The possibility of producing butanol from syngas opens a path to the fully biotechnological production of propene from carbon dioxide and renewable power, thus offering actually sustainable propene production independent of the food versus fuel debate. Nevertheless, the optimal setup of such a cascade, which does not require external reducing power, remains to be determined. This work is a case study of novel cascade systems for the production of propene from *n*-butanol, which could find an industrial application in the future.

Results and Discussion

In initial tests, we used a H_2O_2-generating enzyme cascade system consisting of an alcohol oxidase from *Pichia pastoris* (*Pp*AOx) and an aldehyde dehydrogenase from *Geobacillus stearothermophilus* (*Gst*AlDH)[36] to achieve oxidation of *n*-butanol to butyric acid in two steps. The last step, the oxidative decarboxylation of the acid to the final product propene, was performed by the cytochrome P450 peroxygenase $OleT_{JE}$, which simultaneously used the H_2O_2 that was produced *in situ* by *Pp*AOx in the first step. To regenerate the NAD^+ cofactor, we decided to use NADH oxidase from *Lactobacillus pentosus* (*Lp*NOx) (Scheme 1: this cascade is indicated by an orange color code in the following figures).[37] By using a water-forming instead of a H_2O_2-forming NOx, we wanted to avoid the accumulation of excessive H_2O_2 concentrations, which often lead to rapid inactivation of enzymes.[38] The whole cascade was performed in a closed headspace glass vial system, so the necessary O_2 was not added separately, but diffused from the ambient air.

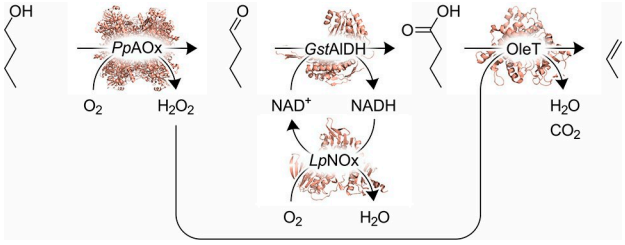

Scheme 1. H_2O_2-dependent enzyme cascade for the production of propene from *n*-butanol by using *Pp*AOx, *Gst*AlDH and OleT. *Lp*NOx is required for the cofactor regeneration.

Initial experiments with the described system were promising but showed only modest amounts of propene (< 5 μM, data not shown). For that reason, we tried to optimize the reaction to obtain higher yields by varying each enzyme concentration (Figure 1). *Pp*AOx and $OleT_{JE}$ had the greatest influence on the cascade, showing a concentration dependent relation. However, excessive *Pp*AOx concentrations resulted in a slightly decreased propene yield (Figure S4 in the Supporting Information), possibly indicating inactivation of the cytochrome P450 active site or other enzymes due to higher amounts of H_2O_2. It is worth mentioning here that Matthews et al. showed a higher H_2O_2 tolerance of $OleT_{JE}$ compared to other bacterial P450 monooxygenases like the fatty acid hydroxylase P450 BM3 heme domain, the *Mycobacterium tuberculosis* P450s CYP51B1 (sterol demethylase) and CYP121 A1 (cyclodipeptide oxidase),

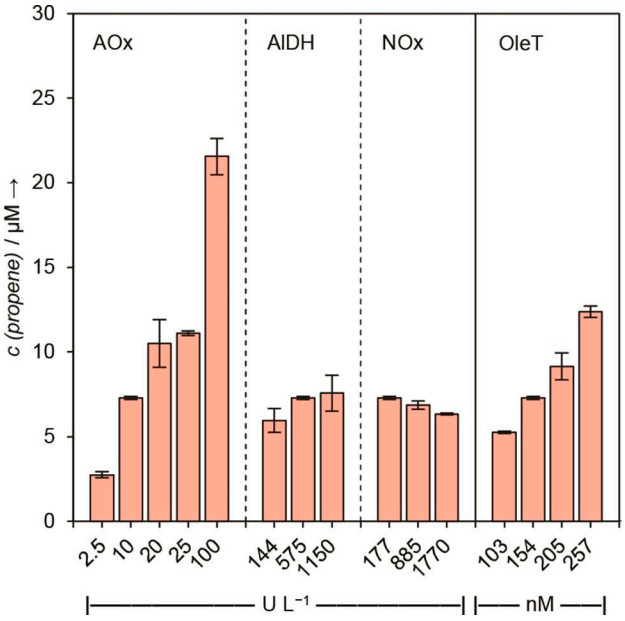

Figure 1. Production of propene at various enzyme concentrations in a H_2O_2-driven cascade. Reaction conditions: 1 mL total reaction volume in a sealed 10 mL headspace glass vial contained 10 U L^{-1} *Pp*AOx, 575 U L^{-1} *Gst*AlDH, 177 U L^{-1} *Lp*NOx, 154 nM $OleT_{JE}$, 200 μM NAD^+, 10 mM *n*-butanol and buffer (50 mM Tris·HCl, pH 7.5). Reactions were performed at 30 °C and 170 rpm for 18 h. Varying *Pp*AOx, *Gst*AlDH, *Lp*NOx or $OleT_{JE}$ concentrations while other conditions remained constant.

which emphasizes its function as a peroxygenase.[19] We further observed that increasing the proportion of $OleT_{JE}$ resulted in an enhanced product formation (Figure S4 and Table S5). Moreover, we figured out that the cascade reaches equilibrium after 5 h until the reaction stops completely after 15 to 18 h (Figure 2).

To prove whether the last oxidation step is actually driven by H_2O_2, we added bovine liver catalase to the system. This experiment was thus initially thought to work as a negative control. To our own surprise, we almost doubled the propene concentrations with catalase present (Figure S5), although we did not expect an increase due to the absence of other redox partners for $OleT_{JE}$. Remarkably, it appears that 200 U mL^{-1} catalase is insufficient for completely removing the peroxide from the system. Similar effects have been reported before.[39,40] A possible explanation is the low affinity towards H_2O_2 of bovine liver catalase, which reaches its full activity at above 50 mM H_2O_2.[41] On the other side a relatively high affinity for H_2O_2 ($K_d = 10.4$ μM)[22] was determined for $OleT_{JE}$.[25] In this case, the catalase solely consumes excess of peroxides, which leads to a reduced enzyme inactivation and, therefore, yields in higher propene amounts. Adding 1000 U mL^{-1} catalase however resulted in decreased yields (Figure S6). The intermediate concentrations showed an accumulation of butyric acid. Due to the high concentration of the present catalase, there is less H_2O_2 left for the oxidative decarboxylation of the acid. It should also be mentioned that *Lp*NOx has a slight catalase activity.[37]

Furthermore, we wanted to find out whether the cascade could be run in a H_2O_2-free system to overcome this issue. Assuming the validity of the theory of $OleT_{JE}$ being a monooxygenase,[10–16] we therefore replaced H_2O_2-producing *Pp*AOx with an alcohol dehydrogenase (ADH). We decided to use ADH from *G. stearothermophilus* (*Gst*ADH), due to its beneficial activity towards *n*-butanol at 30 °C (data not shown). As already shown by other groups, $OleT_{JE}$ is also able to work in a monooxygenase-like setup, using O_2 as an oxidant and NAD(P)H as an electron donor. A wide range of potential redox partner systems have been investigated for $OleT_{JE}$.[10,11,15,16] In our case, we used the well-known redox partners putidaredoxin reductase (PdR) and putidaredoxin (Pdx) from *Pseudomonas putida*, which acted simultaneously as a cofactor regeneration system for *Gst*ADH and *Gst*AlDH as well as an electron transfer system for $OleT_{JE}$ (Scheme 2: this cascade is indicated by a blue color code in the following figures). Similar to the H_2O_2-driven cascade, the reactions were performed in closed headspace glass vials with no external addition of O_2.

Like the H_2O_2-dependent system, initial tests for the NAD(H)-dependent system were successful, so we followed up on the optimization by varying the concentrations of the reaction partners (Figure 3).

Although the first reaction step by *Gst*ADH had no significant influence according to the enzyme concentration, the second reaction step depended more on the *Gst*AlDH concentration. We also varied the ratio and concentration of the $OleT_{JE}$ redox partners PdR and Pdx, showing that a 1:10 μM (PdR/Pdx) ratio worked well for the system. PdR and Pdx are not the natural redox partners for $OleT_{JE}$, so it is more likely that the electron transfer from the NADH cofactor to the cytochrome P450 enzyme is not ideal and goes via rate-limiting decoupling processes. Therefore, higher concentrations of the redox partners can promote a better electron supply. Nevertheless, even higher Pdx concentrations do not seem applicable in our point of view. The cofactor NAD^+ had no significant influence above a concentration of 100 μM. As expected, using the system without catalase raised the yield of propene by 80–100%. This is due to H_2O_2, which was generated by the uncoupling of the cytochrome P450 catalytic cycle[39,40] and which is supposed to be used by the decarboxylase. The production of H_2O_2 by flavin (e.g., from the flavoprotein PdR) in the presence of O_2 is also possible.[17,42]

However, upon comparing the H_2O_2- and NAD(H)-driven cascades, both systems seemed to be affected by H_2O_2. Whereas the former favors the presence of catalase to get rid of excesses of H_2O_2, the latter is best when supported by a certain amount of H_2O_2, thus making it a H_2O_2- and NAD(H)-driven system. Most likely, the cascade can circumvent shortages in electron supply either by H_2O_2 or by the NADH cofactor, depending on the most favored path for the enzymes. This raises the possibility

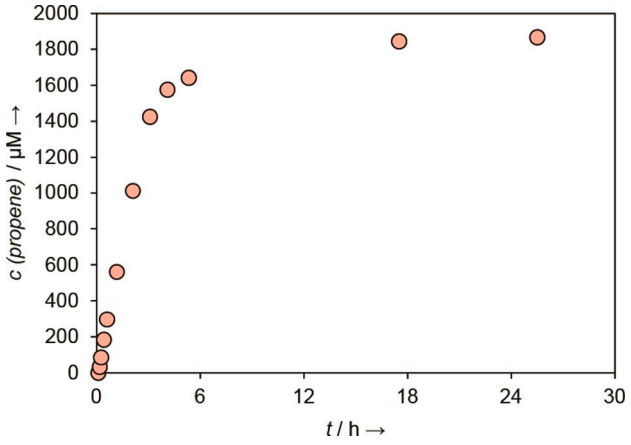

Figure 2. Propene production over time in a H_2O_2-driven system. Reaction conditions: 1 mL total reaction volume in a sealed 10 mL headspace glass vial contained 127 U L^{-1} *Pp*AOx, 575 U L^{-1} *Gst*AlDH, 177 U L^{-1} *Lp*NOx, 5.6 mg mL^{-1} $OleT_{JE}$, 200 μM NAD^+, 10 mM *n*-butanol and buffer (50 mM KPi, pH 7.5). Reactions were performed at 30 °C and 170 rpm for 26 h.

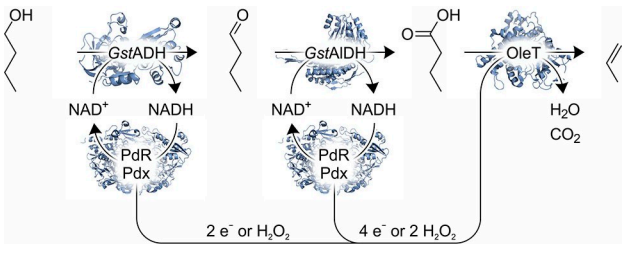

Scheme 2. Potential monooxygenase-like setup of the NAD(H)-dependent enzyme cascade to produce propene from *n*-butanol by using *Gst*ADH, *Gst*AlDH and OleT. PdR and Pdx are required for cofactor regeneration and the electron transfer to OleT. Additionally, H_2O_2 can result from the autoxidation of the redox donor or the formation of superoxide by OleT-oxy complex.[17] OleT uses only two of four electrons per reaction.

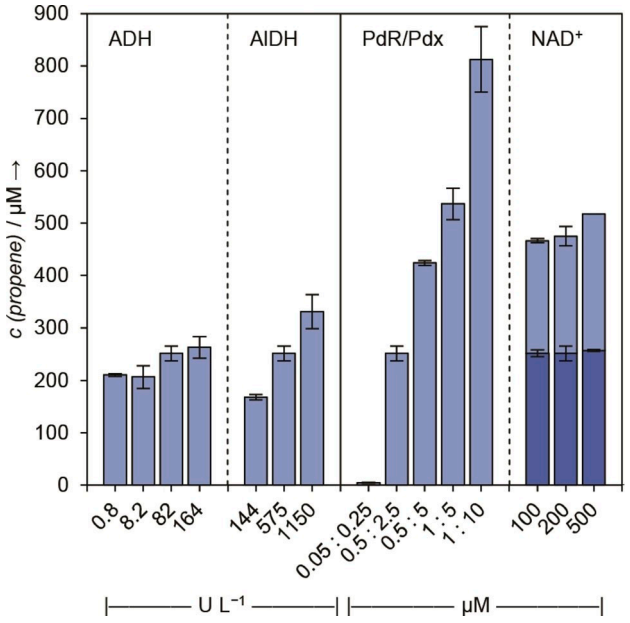

Figure 3. Production of propene at various enzyme concentrations in the NAD(H)-driven cascade. Reaction conditions: 1 mL total reaction volume in a sealed 10 mL headspace glass vial contained 82 U L^{-1} *Gst*ADH, 575 U L^{-1} *Gst*AlDH, 0.5 µM PdR, 2.5 µM Pdx, 0.44 mg mL^{-1} $OleT_{JE}$, 200 U mL^{-1} catalase, 200 µM NAD^+, 10 mM *n*-butanol and buffer (50 mM Tris·HCl, pH 7.5). Reactions were performed at 30 °C and 170 rpm for 18 h. Varying *Gst*ADH, *Gst*AlDH, PdR/Pdx or NAD^+ (with 200 U mL^{-1} (▪) or without (▫) catalase) while other conditions remained constant.

that $OleT_{JE}$ actually only works as a peroxygenase and, if any, additionally together with putidaredoxin as a NADH oxidase. Recent studies support these facts by showing the production of H_2O_2 as a result of autoxidation, either of the redox cofactor, the oxy-ferrous complex or from pyridine nucleotide itself.[17]

Given this knowledge and the optimization achieved thus far, we wanted to improve the cascade by focusing on the last step, the oxidative decarboxylation. As $OleT_{JE}$ predominantly decarboxylates medium- to long-chain fatty acids (C_{12}–C_{20}), butyric acid (C_4) might not bind optimally to the enzyme. We therefore tried to optimize the active site as well as the substrate tunnel to make it more suitable for short-chain fatty acids like butyric acid.

In a first step, we were looking for key amino acid positions that could have a positive influence on the substrate pocket. According to the work of Du et al. the most influential residues are Leu70, Phe173, Val292, Phe296 and Ile402. Changing these residues to ones with larger side chains will shrink the volume of the binding pocket and make a conversion of shorter fatty acids much more favorable;[43] this might have an influence on the decoupling activity. We widened this spectrum using other residues, which might also have an influence on the binding pocket, the substrate channel, the substrate positioning, the decarboxylation activity or polarization (e.g., the proposed key residues Phe79, His85 and Ile170).[15,18,26,27,44] To do so, we focused on amino acids within a radius of 5 Å from the ligand. We neglected the residues near the entrance of the substrate channel, expecting their impact on the occlusion of the substrate close to the area of the binding pocket to be only marginal. The remaining residues were selected according to their structural position and, therefore, their resulting potential influences on the substrate (Figure 4A). Based on the model, Leu78 lies near the chain end of bound butyric acid and might have a stabilization effect by narrowing the tunnel in addition to a catalytic influence when changing the amino acid (e.g., to His). Ile74 is located near the tunnel, indicating its mutation capability for narrowing the substrate channel, which could lead to a higher dwell time of the substrate in the binding pocket. Phe291 could be a potential key residue for an alternative channel for short-chained substrates, providing opportunities to narrow or widen the channel by mutation.[14] Phe79 mutants have already been tested by Matthews et al., but only for C_{10}–C_{20} fatty acids.[18] However, we wanted to investigate this residue for butyric acid.

In our screening, four mutants showed marginal to significant improvements concerning the production of propene (Figure 4D). In particular, the mutants with small improving effects were His85Gln, Ile84Val and the double mutant Val292Ile/Ile170Val. Val292Ile, the most promising mutant, showed a doubling of the yield in comparison with the wild type. Five mutants (Phe79Leu, Ile402Met, Ile170Val, Ala83Gly, Phe173Trp) showed up to 50% lower turnovers than the wild-type enzyme. The rest of the mutants showed only negligible activities. Earlier studies of other groups predicted[22,45] and also showed[15,26] worse conversion towards terminal alkenes for $OleT_{JE}$ His85 mutants due to the histidine's postulated role as a proton donor in the decarboxylation reaction. In any case, Matthews et al. showed in their catalytic studies that His85Gln still favored decarboxylation reaction similar to the wild type;[18] this is confirmed by our results. Also, other CYP152 enzymes like $P450_{BS\beta}$ from *B. subtilis* as well as CYP_{MP} from *M. populi* lacking the His85 (Gln85 in $P450_{BS\beta}$, Met96 in CYP_{MP}) showed decarboxylation activity besides the predominantly catalyzed hydroxylation of fatty acids.[9,32] We had achieved similar results in our own previous studies, but with lower alkene production compared to the wild-type enzyme and increased α-hydroxylation (data not shown), indicating that His85 is important but not essential for the decarboxylation reaction of fatty acids.

To validate and investigate our results further, we decided to compare the best mutant $OleT_{V292I}$ and $OleT_{H85Q}$ in their purified form with the wild type under screening and cascade conditions. We were able to reproduce our results from the screening when using both mutants $OleT_{V292I}$ and $OleT_{H85Q}$ as well as wild-type $OleT_{JE}$ in purified form (Figure 5A). $OleT_{V292I}$ produced almost twice the amount of propene as $OleT_{H85Q}$ and wild type, which produced nearly the same amount of propene. The same tendency was shown when using those variants for the H_2O_2-driven cascade (Figure 5B). At this point, $OleT_{V292I}$ reached TTNs of 1099 and produced 140% more propene than the wild-type enzyme or $OleT_{H85Q}$ mutant, which both again yielded nearly the same amount of propene (1.5–1.8 mM) and only reached TTNs lower than 460. Using the NAD(H)-driven system resulted in an overall reduced product yield for all variants since we added catalase to prove again the sole peroxygenase activity (Figure 5C). Interestingly, within this

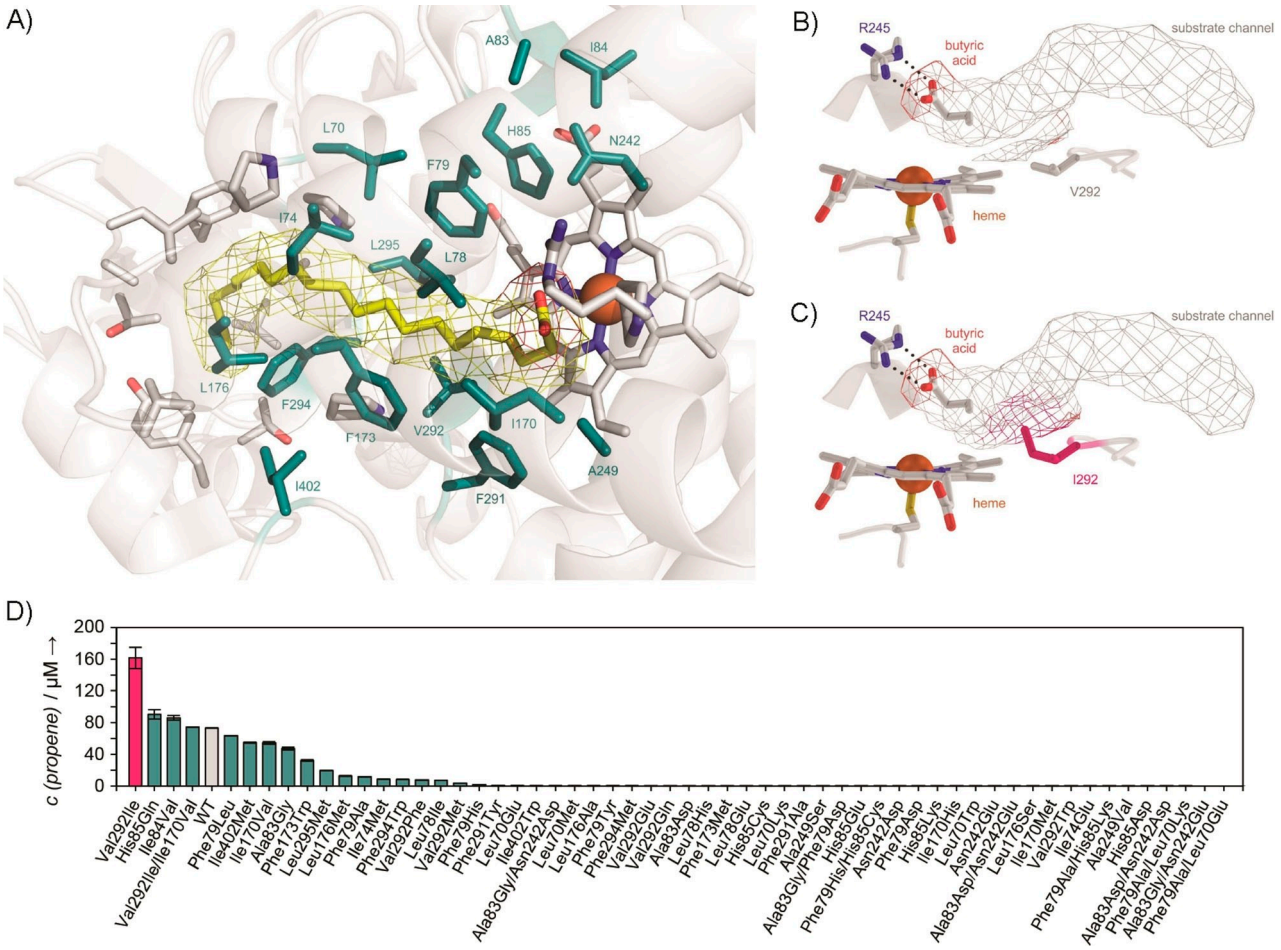

Figure 4. A) Active site and substrate tunnel (yellow, arachidic acid) of wild-type $OleT_{JE}$ (PDB ID: 4L40)[22], highlighting all amino acid residues of our mutation studies (teal). Active site with binding pocket of B) wild-type $OleT_{JE}$ and C) mutant $OleT_{Val292Ile}$: The mutation of Val292 (B: gray residue) to Ile292 (C: pink residue) shrinks the substrate pocket volume, making it more favorable for the binding of short-chain fatty acids like butyric acid. D) Mutation landscape. Reaction conditions: 1 mL total reaction volume in a sealed 10 mL headspace glass vial contained 3 U L^{-1} *Pp*AOx, 2.25 mg mL^{-1} $OleT_{JE}$ crude cell extract (every approach for each $OleT_{JE}$ variant was adapted to the same final crude cell extract concentration of 2.25 mg mL^{-1}), 5 mM methanol, 10 mM butyric acid and buffer (50 mM KPi, pH 7.5). Reactions were performed at 30 °C and 170 rpm for 15 h. Methanol and butyric acid are the standard substances for the enzyme activity assay. The assay consists of the oxidative decarboxylation of butyric acid by $OleT_{JE}$ with H_2O_2 as substrate. H_2O_2 is formed *in situ* by *Pp*AOx with methanol as substrate. The focus of this experiment was not the cascade but solely activity screening for $OleT_{JE}$. Figures were rendered with PyMol after minimization in YASARA by using the Amber99 force field.

system $OleT_{V292I}$ only showed marginal improvements in comparison to the wild type, whereas $OleT_{H85Q}$ showed a strong decrease in propene yield. The clear decrease in product yield for $OleT_{H85Q}$ using the NAD(H)-dependent system led us to believe that both mutants show higher activity in the presence of H_2O_2, while the interaction with the redox partners is not as effective as for the wild-type enzyme. This could be due to conformational changes near the active site as a result of the mutations. However, it remains unclear why the NAD(H)-dependent system did not work as well as the H_2O_2-driven cascade for both OleT variants.

Examination of the active site of our mutant $OleT_{V292I}$ reveals a hypothetical reason for the increased product yield in comparison to the wild-type enzyme. As Du et al. postulated in their calculations,[43] the exchange of valine to the larger isoleucine caused a narrowing of the substrate tunnel and the binding pocket (Figure 4B and C). This probably led to a more effective binding and stabilization of the short-chained butyric acid, resulting in higher yields of propene. Interestingly, the recently characterized peroxygenases CYP152K6 from *Bacillus methanolicus* MGA3[46] and CYP152N1 from *Exiguobacterium* sp. ATIb[47] have a phenylalanine at the equivalent V292 position in $OleT_{JE}$, most likely inducing a structural kink in the alkyl chain of the tetradecanoic acid substrate relevant to the hydroxylation reaction. Similar to the Phe292 residue in CYP152K6 and CYP152N1, the Ile292 residue in $OleT_{V292I}$ occupies and narrows the space between the heme and the substrate channel. In our case, the narrowing seems to be more important for enclosing the short-chain substrate. We did not detect any side products like hydroxybutyric acids, which supports the finding of Dennig et al., who were also unable to detect hydroxy acids.[11] Furthermore, we only detected none or marginal amounts of the intermediate butanal of up to a maximum of 880 µM (Figures S6 and S7), depending on the $OleT_{JE}$ concentration.

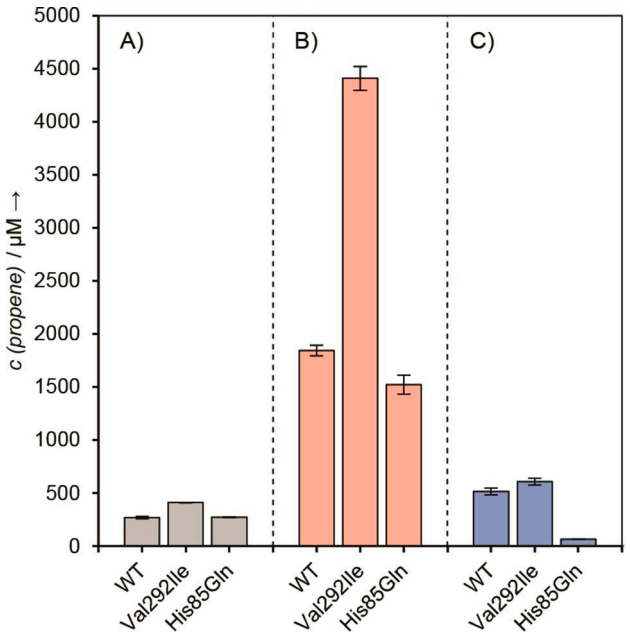

Figure 5. Production of propene with $OleT_{JE}$ wild type and mutants Val292Ile and His85Gln. A) Comparison under screening conditions. Reaction conditions: 1 mL total reaction volume in a sealed 10 mL headspace glass vial contained 3 U L^{-1} *Pp*AOx, 1.16 µM $OleT_{JE}$ variant (every approach for each $OleT_{JE}$ variant was adapted to the same final concentration), 15 mM methanol, 10 mM butyric acid and buffer (50 mM Tris·HCl, pH 7.5). Reactions were performed at 30 °C and 170 rpm for 18 h. B) Comparison of H_2O_2-driven cascades. Reaction conditions: 1 mL total reaction volume in a sealed 10 mL headspace glass vial contained 127 U L^{-1} *Pp*AOx, 575 U mL^{-1} *Gst*AlDH, 177 U mL^{-1} *Lp*NOx, 4.01 µM $OleT_{JE}$ variant (every approach for each $OleT_{JE}$ variant was adapted to the same final concentration), 200 µM NAD^+, 10 mM *n*-butanol and buffer (50 mM Tris·HCl, pH 7.5). Reactions were performed at 30 °C and 170 rpm for 18 h. C) Comparison of NAD(H)-driven cascades. Reaction conditions: 1 mL total reaction volume in a sealed 10 mL headspace glass vial contained 82 U L^{-1}*Gst*ADH, 575 U L^{-1}*Gst*AlDH, 1 µM PdR, 10 µM Pdx, 4.01 µM $OleT_{JE}$ variant (every approach for each $OleT_{JE}$ variant was adapted to the same final concentration), 1000 U mL^{-1} catalase, 200 µM NAD^+, 10 mM *n*-butanol and buffer (50 mM Tris·HCl, pH 7.5). Reactions were performed at 30 °C and 170 rpm for 18 h.

Conclusion

In summary, both *in vitro* cascades provide a first promising basis as a practical means for producing the relevant bulk chemical propene from *n*-butanol, which can be derived from renewable resources. However, we found strong indications that $OleT_{JE}$ mainly works as a peroxygenase. With the help of enzyme engineering, we produced the mutant $OleT_{V292I}$, which showed an almost 250% production rate compared to the wild type. To the best of our knowledge the highest conversion so far for propene production with $OleT_{JE}$ was reported to be 5%.[11] Using our improved system and our new variant, we were able to increase the alkene production almost tenfold. Focusing on further enzyme mutations will be one key element for future studies aiming in enhancing the yield of the cascades. Therefore, suitable high-throughput screening systems, like a recently established one for detecting the conversion of medium-chain fatty acids by $OleT_{JE}$,[48] could play an essential role in reducing the screening effort.

Experimental Section

Materials: All chemicals, if not stated otherwise, were purchased from Sigma-Aldrich or Carl Roth. Alcohol oxidase from *P. pastoris* (*Pp*AOx, 21 U mg^{-1}) was obtained from Sigma-Aldrich; one unit will oxidize 1.0 µmol methanol to formaldehyde per min at pH 7.5 and 25 °C. Lysozyme from egg white (≥ 35000 FIP U mg^{-1}) was obtained from Carl Roth; one FIP unit equates the protein concentration that induces a reduction of the extinction of 0.001 per min at 450 nm, pH 7.0 and 25 °C, using a solution of *Micrococcus luteus* as substrate. DNase I (4 U mg^{-1}) was obtained from AppliChem GmbH (Darmstadt, Germany).

Cloning: The cloning of the expression plasmid pET-28a_*gst*ADH (pET-28a(+) vector carrying the *Gst*ADH gene from *G. stearothermophilus* with N-terminal His tag) was described previously.[3] The cloning of the expression plasmid pET-28_*gst*AlDH (pET-28a(+) vector carrying the *Gst*AlDH gene from *G. stearothermophilus* with C-terminal His tag) was described previously.[36] The cloning of the expression plasmid pET-28a_*lp*NOx (pET-28a(+) vector carrying the *Lp*NOx gene from *L. pentosus* with N-terminal His-tag) was described previously.[37] The expression plasmid pASK_oleT (pASK-IBA37plus vector carrying the $OleT_{JE}$ gene from *Jeotgalicoccus* sp. ATCC 8456) was provided by Robert Kourist (Ruhr University Bochum, Germany).[21] The cloning of the expression plasmid pET-22b_PdR (pET-22b(+) vector carrying the PdR gene from *P. putida* with C-terminal His tag) was described previously.[49,50] The cloning and site-directed mutagenesis of the expression plasmid pET-22b_Pdx (pET-22b(+) vector carrying the $Pdx_{C73S/C85S}$ gene from *P. putida* with C-terminal His tag) was described previously.[49,50] $OleT_{JE}$ mutants were produced by QuikChange mutagenesis. The primers were ordered from Eurofins Genomics (Table S1). Reactions (50 µL) contained 10 µL Phusion® HF buffer (5×, New England BioLabs, Ipswich, MA, USA), 10 µL dNTP Mix (each 10 mM), 1 µL forward primer (10 µM), 1 µL reverse primer (10 µM), 20 ng template (pASK_OleT for single mutants, $OleT_{JE}$ single mutant plasmids for double mutants), 5 µL DMSO, 1 µL Phusion® High-Fidelity DNA Polymerase (2000 U mL^{-1}, New England BioLabs) and ddH_2O. Reactions were thermocycled as followed: 98 °C for 2 min (step 1); 98 °C for 30 s, 57–64 °C for 1 min, 72 °C for 3 min (step 2, 16×); 72 °C for 10 min (step 3) and 4 °C for storage. Afterwards each sample was digested overnight with 1 µL DpnI (20000 U mL^{-1}, New England BioLabs) at 37 °C. The DNA was purified using the NucleoSpin® Gel and PCR Clean-up Kit (Merchery-Nagel) as described in the manual. *Escherichia coli* BL21(DE3) cells were chemically transformed with 10 µL of each purified $OleT_{JE}$ mutant DNA (50–80 ng $µL^{-1}$), before they were grown overnight on lysogeny broth (LB) agar medium supplemented with 100 µg mL^{-1} ampicillin. Three clones were randomly selected and sequenced from plasmid DNA using the forward or reverse primer (Eurofins Genomics, Ebersberg, Germany).

Enzyme expression: A detailed list of the expression conditions (cells, plasmids, media, supplements, antibiotics, incubation temperatures) for the individual enzymes can be found in Table S2. Cells were chemically transformed with plasmids, before they were grown overnight on LB agar plates supplemented with antibiotic. 20 mL liquid medium with antibiotic in an 100 mL Erlenmeyer shaking flask were inoculated with one colony and incubated overnight at 150 rpm on a rotary shaker. Part of this preculture was used to inoculate the main culture in a 5 L Erlenmeyer shaking flask. The main culture was incubated at 110 rpm on a rotary shaker for 16 h–24 h. The cells were harvested by centrifugation (5000 *g*, 15 min, 4 °C) and stored at −20 °C.

Enzyme purification: All protein purification steps were carried out at room temperature using an ÄKTA™ UPC-900 FPLC system (GE Healthcare). All buffers (Table S3) were filtered with 0.2 µm

regenerated cellulose membranes (VWR International, Radnor, USA).

Purification of *Gst*ADH, *Gst*AlDH, *Lp*NOx, PdR and Pdx: The cells were thawed and resuspended to a 10% (*w*/*v*) (20% *w*/*v* for PdR and Pdx) solution in binding buffer. The cell disruption was carried out once (twice for PdR and Pdx) using a French press (Basic-Z Cell Disrupter, IUL Constant Systems, Northants, UK) at 1.37 kbar. DNase I (1 μg mL^{-1}) and $MgCl_2$ (2.5 mM) were added to the cell lysate (additionally FAD (50 μM) for *Lp*NOx and lysozyme (5 mg mL^{-1}) for PdR and Pdx), and the solution was incubated for 25 min at room temperature on a rocking shaker. The cell debris was removed afterwards by centrifugation (35 000 *g*, 45 min, 4 °C). The remaining crude extract was filtered through a syringe filter (0.45 μm, VWR International), before it was loaded on a 5 mL HisTrap™ FF column (GE Healthcare), which was preliminary equilibrated with binding buffer. After removing *E. coli* proteins by washing the column with five column volumes binding buffer, protein was eluted by using a gradient from 0% to 100% elution buffer. Eluted fractions were subjected to 12% SDS-PAGE.[51] The molecular weight of the desired protein was calculated by using the ExPASy ProtParam tool (Table S4).[52] Fractions with the protein were pooled and desalted using a HiPrep™ 26/10 Desalting column (GE Healthcare), which was preliminary equilibrated with desalting buffer. Pooled fractions of the protein (mixed with 1 mM DTT for PdR and Pdx) were frozen in liquid nitrogen and stored at −80 °C.

Purification of OleT$_{JE}$ and mutants: The cells were thawed and resuspended to a 10% (*w*/*v*) solution in binding buffer supplemented with small amounts of lysozyme, 1 μg mL^{-1} DNase I and 2.5 mM $MgCl_2$. The incubation for 2 h at room temperature was followed by cell disruption with a French press (Basic-Z Cell Disrupter, IUL Constant Systems, Northants, UK) at 1.37 kbar. The cell debris was removed afterwards by centrifugation (35 000 *g*, 45 min, 4 °C). The remaining crude extract was filtered through a syringe filter (0.45 μm, VWR International) before it was loaded on a 5 mL HisTrap™ FF column (GE Healthcare), which was preliminary equilibrated with binding buffer. After removing *E. coli* proteins by washing the column with five column volumes binding buffer, protein was eluted by using a gradient of 50% binding buffer and 50% elution buffer. Eluted fractions were subjected to 12% SDS-PAGE (Figure S1).[51] The molecular weight of the desired protein was calculated using the ExPASy ProtParam tool.[52] Fractions with the protein were pooled and dialyzed (3×12 h) against 50 times excess of dialysis buffer at 4 °C to remove imidazole. The purified protein was stored at 4 °C (Figure S8).

Determination of protein concentration: The protein concentrations were determined using the Bradford assay Roti®-Quant (Carl Roth) with BSA as standard, following the instructions for the microassay. In addition, some concentrations were measured at 280 nm using NanoPhotometer® P 330 (Implen, Munich, Germany) with parameters under reduced conditions (Table S4). Reduction was achieved by diluting the enzyme 1:1 with 12 M guanidine hydrochloride.

CO difference spectroscopy: The amount of active OleT$_{JE}$ was determined using CO difference spectroscopy.[53] 90 μL of the protein in a microtiter plate were diluted with 70 μL KPi (100 mM, pH 7.5) and 40 μL CO buffer (1.3 mM KPi, 400 mM $Na_2S_2O_4$, pH 8.0), either treated with CO gas for 5 min or not. The samples were measured with the FLUOstar® Omega (BMG Labtech, Ortenberg, Germany) at 400–500 nm before the concentration of active enzyme was calculated by the differences of the absorption A from the CO-treated sample and the untreated sample (for standardization, the absorption value at 490 nm was subtracted from the absorption value at 450 nm). Protein concentrations measured with CO difference spectroscopy are given in nanomolar or micromolar. When no CO difference spectroscopy was possible (due to facility reasons), the OleT$_{JE}$ concentration was determined by Bradford assay or with the NanoPhotometer® P 330 (Implen), taking into account that not all OleT$_{JE}$ protein was fully loaded. These values are given in mg mL^{-1}. Results across experiments with different mg mL^{-1} values are not comparable.

Catalytic approach: Biocatalysis was done in two types of three-step cascades, either depending on H_2O_2 or NAD(H). Reactions were performed at 30 °C and 170 rpm for 18 h before being stopped by heating the samples to 80 °C for 10 min. The samples were then analyzed by GC-FID and GC-MS. In preparation for the HPLC measurements, the aqueous phase was spin filtrated at 14 000 *g* for 15 min (centrifugal filter, modified PES, 10K, VWR International) after finishing the GC measurements.

H_2O_2-driven catalysis: A typical reaction approach consists of 1 mL total reaction volume with 127 U L^{-1} *Pp*AOx, 575 U L^{-1} *Gst*AlDH, 177 U L^{-1} *Lp*NOx, a maximum of 50% (*v*/*v*) OleT$_{JE}$ (see captions), 200 μM NAD^+, 10 mM *n*-butanol and buffer (50 mM Tris·HCl, pH 7.5) in a sealed 10 mL headspace glass vial (Macherey-Nagel). No O_2 was added separately.

NAD(H)-driven catalysis: A typical reaction approach consists of 1 mL total reaction volume with 82 U L^{-1} *Gst*ADH, 575 U L^{-1} *Gst*AlDH, 0.5 μM PdR, 2.5 μM Pdx, a maximum of 50% (*v*/*v*) OleT$_{JE}$ (see captions), 200 U mL^{-1} catalase, 200 μM NAD^+, 10 mM *n*-butanol and buffer (50 mM Tris·HCl, pH 7.5) in a sealed 10 mL headspace glass vial (Macherey-Nagel). No O_2 was added separately.

Screening for suitable OleT$_{JE}$ mutants: *E. coli* BL21(DE3) cells were chemically transformed with 5 μL of each purified OleT$_{JE}$ mutant DNA (50–80 ng μL^{-1}), before they were grown overnight on LB agar medium supplemented with 100 μg mL^{-1} ampicillin. Two clones of each mutant were randomly selected to inoculate 2×1 mL LB medium with 50 μg mL^{-1} ampicillin in a 96 deep-well plate (DWP) and incubated overnight at 37 °C and 800 rpm on a plate shaker. These precultures were combined for each mutant and used to inoculate 8×5 mL expression medium (900 mL TB medium, 100 mL 10×KPi solution, 250 μL trace element solution, 50 μg mL^{-1} ampicillin) for each mutant in a 24 DWP, using 210 μL preculture per 5 mL well. The main cultures were incubated at 37 °C and 800 rpm on a rotary shaker until an $OD_{600\,nm}$ of 0.7–0.8, before they were supplemented with 500 μM δ-aminolevulinic acid, induced with 0.2 mg L^{-1} anhydrotetracycline hydrochloride and incubated at 18 °C and 800 rpm for additional 24 h. The cells were harvested by centrifugation (4500 *g*, 15 min, 4 °C) and resuspended in 750 μL resuspension buffer (100 mM KPi, 300 mM NaCl, pH 7.5). The cells of same mutants were combined and centrifuged again (4500 *g*, 15 min, 4 °C), before they were stored at −20 °C.

The cells were thawed and resuspended in 3 mL desalting buffer (100 mM KPi, 750 mM NaCl, 20% (*v*/*v*) glycerol, pH 8.0) before being treated with ultrasound (Sonoplus, BANDELIN and Hielscher LS24d10, 3×45 s with 45 s breaks, 70% amplitude, 0.5 cycle). The cell debris was removed afterwards by centrifugation (35 000 *g*, 45 min, 4 °C). The protein concentration of the supernatant was determined using the Bradford assay. For the subsequent assay, the protein concentrations were adjusted to the lowest concentration of all mutants in order to obtain uniform protein amounts for each sample. 1 mL total reaction volume in a sealed 10 mL headspace glass vial (Macherey-Nagel) contained 3 U L^{-1} *Pp*AOx, a maximum of 50% (*v*/*v*) OleT$_{JE}$ crude cell extract, 5 mM methanol, 10 mM butyric acid and buffer (50 mM KPi, pH 7.5). No O_2 was added separately. Reactions were performed at 30 °C and 170 rpm for 15 h before being stopped by heating the samples to 80 °C for 10 min. The samples were then analyzed by GC-FID.

GC-FID: Qualitatively and quantitatively analysis of propene formation was carried out by gas chromatography using a Rt®-QS-BOND column (15 m by 0.53 mm, 20 μm film, Restek GmbH, Bad Homburg, Germany) on a TRACE™ 1310 gas chromatograph (Thermo Scientific) with a FID detector. The samples were incubated at 40 °C for 1 min before 1 mL of the gaseous phase was injected (syringe temperature: 50 °C) and separated on the column (inlet and detector 200 °C, 40 °C/hold 1 min, 10 °C min^{-1} to 50 °C/hold 0 min, 40 °C min^{-1} to 150 °C/hold 4 min). Airgas standards (C_2–C_6 olefins, Restek) were used for identification of propene (t_R = 3.357 min) and preparation of calibration curves (Figure S2).

GC-MS: Analysis of *n*-butanol, butyraldehyde and propene (Figure S3) was carried out using Rxi®-5Sil-MS column (60 m by 0.53 mm, 20 μm film, Restek) on a TRACE™ GC Ultra gas chromatograph (Thermo Scientific) with a Quadrupol detector. The samples were incubated at 40 °C for 1 min before 1 mL of the gaseous phase was injected (syringe temperature: 50 °C) and separated on the column (inlet and detector 200 °C, 40 °C/hold 1 min, 10 °C min^{-1} to 50 °C/hold 0 min, 40 °C min^{-1} to 150 °C/hold 4 min).

HPLC: HPLC analytics were done according to previous methods.[54] The concentrations of *n*-butanol, butyraldehyde and butyric acid in the aqueous solutions were quantified using a HPLC system (Dionex™, Sunnyvale, CA, USA) equipped with a Rezex™ ROA-H^+ column (Phenomenex, Torrance, CA, USA), a refractive index detector (RI 101, Shodex™, Tokyo, Japan) and a PDA detector (210 nm, Dionex™). The mobile phase (sulfuric acid, 2.5 mM) was set to a flow rate of 0.5 mL min^{-1} at an oven temperature of 70 °C. Prior to measurement, all samples were filtered through a 0.2 μm PVDF filter (Restek). Qualitative analyses and quantitative calculations of each compound were referred to an external standard of *n*-butanol (t_R = 42.404 min), butyraldehyde (t_R = 34.737 min) and butyric acid (t_R = 25.588 min).

Acknowledgements

The authors acknowledge financial support from the German Federal Ministry of Education and Research (BMBF) for Daniel Bauer (grant no. 03SF0446A) and Ioannis Zachos (grant no. 031A177B). We thank Prof. Dr. Robert Kourist for providing the plasmid pASK oleT, and Dr. Michael Hofer and Steffen Roth for providing the plasmids pET-22b_PdR and pET-22b_Pdx. Open access funding enabled and organized by Projekt DEAL.

Conflict of Interest

The authors declare no conflict of interest.

Keywords: biocatalysis · butanol · enzyme engineering · P450 fatty acid decarboxylase · propene · syngas

[1] a) R. A. Kerr, *Science* **2007**, *316*, 188–190; b) G. Stephanopoulos, *Science* **2007**, *315*, 801–804.
[2] H. Li, A. F. Cann, J. C. Liao, *Annu. Rev. Chem. Biomol. Eng.* **2010**, *1*, 19–36.
[3] J.-K. Guterl, D. Garbe, J. Carsten, F. Steffler, B. Sommer, S. Reiße, A. Philipp, M. Haack, B. Rühmann, A. Koltermann et al., *ChemSusChem* **2012**, *5*, 2165–2172.
[4] a) S. Reiße, M. Haack, D. Garbe, B. Sommer, F. Steffler, J. Carsten, F. Bohnen, V. Sieber, T. Brück, *Front. Bioeng. Biotechnol.* **2016**, *4*, 703; b) P. Dürre, *Biotechnol. J.* **2007**, *2*, 1525–1534.
[5] a) M. Sjöblom, L. Matsakas, P. Christakopoulos, U. Rova, *FEMS Microbiol. Lett.* **2016**, *363*, fnw064; b) J. O. Metzger, U. Bornscheuer, *Appl. Microbiol. Biotechnol.* **2006**, *71*, 13–22.
[6] D. Sorigué, B. Légeret, S. Cuiné, S. Blangy, S. Moulin, E. Billon, P. Richaud, S. Brugière, Y. Couté, D. Nurizzo et al., *Science* **2017**, *357*, 903–907.
[7] Z. Rui, X. Li, X. Zhu, J. Liu, B. Domigan, I. Barr, J. H. D. Cate, W. Zhang, *Proc. Natl. Acad. Sci. USA* **2014**, *111*, 18237–18242.
[8] Z. Rui, N. C. Harris, X. Zhu, W. Huang, W. Zhang, *ACS Catal.* **2015**, *5*, 7091–7094.
[9] M. A. Rude, T. S. Baron, S. Brubaker, M. Alibhai, S. B. Del Cardayre, A. Schirmer, *Appl. Environ. Microbiol.* **2011**, *77*, 1718–1727.
[10] Y. Liu, C. Wang, J. Yan, W. Zhang, W. Guan, X. Lu, S. Li, *Biotechnol. Biofuels* **2014**, *7*, 28.
[11] A. Dennig, M. Kuhn, S. Tassoti, A. Thiessenhusen, S. Gilch, T. Bülter, T. Haas, M. Hall, K. Faber, *Angew. Chem. Int. Ed.* **2015**, *54*, 8819–8822.
[12] A. Dennig, S. Kurakin, M. Kuhn, A. Dordic, M. Hall, K. Faber, *Eur. J. Org. Chem.* **2016**, *2016*, 3473–3477.
[13] A. Dennig, A. Thiessenhusen, S. Gilch, T. Haas, M. Hall, *BIOspektrum* **2016**, *22*, 614–616.
[14] J.-b. Wang, R. Lonsdale, M. T. Reetz, *Chem. Commun.* **2016**, *52*, 8131–8133.
[15] B. Fang, H. Xu, Y. Liu, F. Qi, W. Zhang, H. Chen, C. Wang, Y. Wang, W. Yang, S. Li, *Sci. Rep.* **2017**, *7*, 44258.
[16] C. Lu, F. Shen, S. Wang, Y. Wang, J. Liu, W.-J. Bai, X. Wang, *ACS Catal.* **2018**, 5794–5798.
[17] C. E. Wise, C. H. Hsieh, N. L. Poplin, T. M. Makris, *ACS Catal.* **2018**, *8*, 9342–9352.
[18] S. Matthews, J. D. Belcher, K. L. Tee, H. M. Girvan, K. J. McLean, S. E. J. Rigby, C. W. Levy, D. Leys, D. A. Parker, R. T. Blankley et al., *J. Biol. Chem.* **2017**, *292*, 5128–5143.
[19] S. Matthews, K. L. Tee, N. J. Rattray, K. J. McLean, D. Leys, D. A. Parker, R. T. Blankley, A. W. Munro, *FEBS Lett.* **2017**, *591*, 737–750.
[20] a) B. Chen, D.-Y. Lee, M. W. Chang, *Metab. Eng.* **2015**, *31*, 53–61; b) J. Yan, Y. Liu, C. Wang, B. Han, S. Li, *Biotechnol. Biofuels* **2015**, *8*, 34; c) F. Li, K. Yang, Y. Xu, Y. Qiao, Y. Yan, J. Yan, *Bioresour. Technol.* **2019**, *272*, 451–457.
[21] I. Zachos, S. K. Gaßmeyer, D. Bauer, V. Sieber, F. Hollmann, R. Kourist, *Chem. Commun.* **2015**, *51*, 1918–1921.
[22] J. Belcher, K. J. McLean, S. Matthews, L. S. Woodward, K. Fisher, S. E. J. Rigby, D. R. Nelson, D. Potts, M. T. Baynham, D. A. Parker et al., *J. Biol. Chem.* **2014**, *289*, 6535–6550.
[23] a) C. H. Hsieh, X. Huang, J. A. Amaya, C. D. Rutland, C. L. Keys, J. T. Groves, R. N. Austin, T. M. Makris, *Biochemistry* **2017**, *56*, 3347–3357; b) C. H. Hsieh, T. M. Makris, *Biochem. Biophys. Res. Commun.* **2016**, *476*, 462–466; c) J. Yang, Q. Nie, H. Liu, M. Xian, H. Liu, *BMC Biotechnol.* **2016**, *16*, 801.
[24] a) S. Bojarra, D. Reichert, M. Grote, Á. G. Baraibar, A. Dennig, B. Nidetzky, C. Mügge, R. Kourist, *ChemCatChem* **2018**, *10*, 1192–1201; b) M. Pickl, S. Kurakin, F. G. Cantú Reinhard, P. Schmid, A. Pöcheim, C. K. Winkler, W. Kroutil, S. P. de Visser, K. Faber, *ACS Catal.* **2019**, *9*, 565–577; c) D. Yu, J.-b. Wang, M. T. Reetz, *J. Am. Chem. Soc.* **2019**, *141*, 5655–5658.
[25] J. A. Amaya, C. D. Rutland, N. Leschinsky, T. M. Makris, *Biochemistry* **2018**, *57*, 344–353.
[26] H. Xu, L. Ning, W. Yang, B. Fang, C. Wang, Y. Wang, J. Xu, S. Collin, F. Laeuffer, L. Fourage et al., *Biotechnol. Biofuels* **2017**, *10*, 2253.
[27] J.-W. Lee, N. P. Niraula, C. T. Trinh, *Metab. Eng. Commun.* **2018**, *7*, e00076.
[28] Y. Jiang, Z. Li, C. Wang, Y. J. Zhou, H. Xu, S. Li, *Biotechnol. Biofuels* **2019**, *12*, 79.
[29] I. Matsunaga, M. Yamada, E. Kusunose, Y. Nishiuchi, I. Yano, K. Ichihara, *FEBS Lett.* **1996**, *386*, 252–254.
[30] I. Matsunaga, A. Ueda, N. Fujiwara, T. Sumimoto, K. Ichihara, *Lipids* **1999**, *34*, 841–846.
[31] M. Girhard, S. Schuster, M. Dietrich, P. Dürre, V. B. Urlacher, *Biochem. Biophys. Res. Commun.* **2007**, *362*, 114–119.
[32] J. A. Amaya, C. D. Rutland, T. M. Makris, *J. Inorg. Biochem.* **2016**, *158*, 11–16.
[33] I. Amghizar, L. A. Vandewalle, K. M. van Geem, G. B. Marin, *Engineering* **2017**, *3*, 171–178.
[34] a) S. Tan, B. Hu, W.-G. Kim, S. H. Pang, J. S. Moore, Y. Liu, R. S. Dixit, J. G. Pendergast, D. S. Sholl, S. Nair et al., *ACS Catal.* **2016**, *6*, 5673–5683; b) A.

Agarwal, D. Sengupta, M. El-Halwagi, *ACS Sustain. Chem. Eng.* **2018**, *6*, 2407–2421.
[35] P. N. R. Vennestrøm, C. M. Osmundsen, C. H. Christensen, E. Taarning, *Angew. Chem. Int. Ed.* **2011**, *50*, 10502–10509.
[36] T. Imanaka, T. Ohta, H. Sakoda, N. Widhyastuti, M. Matsuoka, *J. Ferment. Bioeng.* **1993**, *76*, 161–167.
[37] C. Nowak, B. Beer, A. Pick, T. Roth, P. Lommes, V. Sieber, *Front. Microbiol.* **2015**, *6*, W597.
[38] K. Hernandez, A. Berenguer-Murcia, R. C. Rodrigues, R. Fernandez-Lafuente, *Curr. Org. Chem.* **2012**, *16*, 2652–2672.
[39] D. P. Nickerson, C. F. Harford-Cross, S. R. Fulcher, L.-L. Wong, *FEBS Lett.* **1997**, *405*, 153–156.
[40] J. A. Fruetel, J. R. Collins, D. L. Camper, G. H. Loew, P. R. Ortiz de Montellano, *J. Am. Chem. Soc.* **1992**, *114*, 6987–6993.
[41] a) G. Ozyilmaz, S. S. Tukel, O. Alptekin, *Indian J. Biochem. Biophys.* **2007**, *44*, 38–43; b) Ö. Alptekin, S. S. Tükel, D. Yıldırım, D. Alagöz, *J. Mol. Catal. B Enzym.* **2010**, *64*, 177–183.
[42] a) V. Massey, *J. Biol. Chem.* **1994**, *269*, 22459–22462; b) K. R. Messner, J. A. Imlay, *J. Biol. Chem.* **2002**, *277*, 42563–42571.
[43] J. Du, L. Liu, L. Z. Guo, X. J. Yao, J. M. Yang, *J. Comput. Aided Mol. Des.* **2017**, *31*, 483–495.
[44] A. S. Faponle, M. G. Quesne, S. P. de Visser, *Chem. Eur. J.* **2016**, *22*, 5478–5483.
[45] J. L. Grant, M. E. Mitchell, T. M. Makris, *Proc. Natl. Acad. Sci. USA* **2016**, *113*, 10049–10054.
[46] H. M. Girvan, H. Poddar, K. J. McLean, D. R. Nelson, K. A. Hollywood, C. W. Levy, D. Leys, A. W. Munro, *J. Inorg. Biochem.* **2018**, *188*, 18–28.
[47] H. Onoda, O. Shoji, K. Suzuki, H. Sugimoto, Y. Shiro, Y. Watanabe, *Catal. Sci. Technol.* **2018**, *8*, 434–442.
[48] H. Xu, W. Liang, L. Ning, Y. Jiang, W. Yang, C. Wang, F. Qi, L. Ma, L. Du, L. Fourage et al., *ChemCatChem* **2019**, *12*, 80–84.
[49] M. Hofer, H. Strittmatter, V. Sieber, *ChemCatChem* **2013**, *5*, 3351–3357.
[50] S. Roth, I. Funk, M. Hofer, V. Sieber, *ChemSusChem* **2017**, *10*, 3574–3580.
[51] U. K. Laemmli, *Nature* **1970**, *227*, 680–685.
[52] P. Artimo, M. Jonnalagedda, K. Arnold, D. Baratin, G. Csardi, E. de Castro, S. Duvaud, V. Flegel, A. Fortier, E. Gasteiger et al., *Nucleic Acids Res.* **2012**, *40*, W597–603.
[53] a) T. Omura, R. Sato, *J. Biol. Chem.* **1964**, *239*, 2379–2385; b) T. Omura, R. Sato, *J. Biol. Chem.* **1964**, *239*, 2370–2378.
[54] H. Hohagen, D. Schwarz, G. Schenk, L. W. Guddat, D. Schieder, J. Carsten, V. Sieber, *Bioresour. Technol.* **2017**, *245*, 1084–1092.

Manuscript received: June 12, 2020
Revised manuscript received: July 9, 2020
Accepted manuscript online: July 12, 2020
Version of record online: August 5, 2020

FULL PAPERS

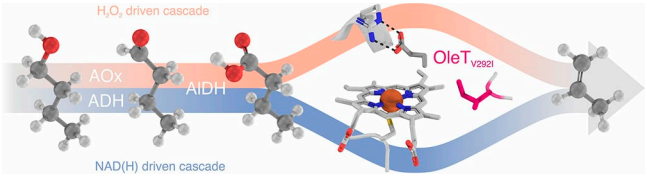

Propelled to propene: Propene is produced in a three-step enzymatic cascade from *n*-butanol via butanal and butyric acid, with the last step being oxidative decarboxylation catalyzed by $OleT_{JE}$. Variation of the supply of redox donors demonstrates the peroxygenase nature of $OleT_{JE}$. A mutational study led to a new variant, $OleT_{V292I}$, which shows significantly higher activity towards the short-chain substrate.